



Full Length Article

Structural Characterization of a Directed Self-Assembly Recombinant Quasi-Spider Silk Protein Expressed in *Escherichia coli*

Bin Liu¹, Tao Wang¹, Liyan Xiao², Yun Li¹, Min Zhu¹, Wanqi Lan¹, Wensun Zhong¹ and Qiang Fu^{1*}

¹Department of Medicine, Jinggangshan University, Jian 343009, China

²School of Foreign Languages, Jinggangshan University, Jian 343009, China

*For correspondence: fqiang9@126.com; yangf@aset.ac.cn

Abstract

Native spider silk protein is an extracellular fibrous protein with distinctive characteristics of elasticity and strength. However, its application was limited for several shortcomings. Here we expressed a recombinant quasi-spider silk protein in which collagen-like peptides were fused to the spider silk protein in *Escherichia coli*. This recombinant protein is a “ABA” type triblock copolymer. Part A which located in both ends of the protein composed of (Pro-Gly-Pro)_n homopolymeric stretches, formed the orientable collagen three-helix structure. While, the intervening block (part B) is the spider silk protein which is optimally designed. Results showed that the interest protein gene was successfully expressed in *Escherichia coli*. Structure characterization of this recombinant protein indicates tremendous potential usage in new biomedical material field. © 2019 Friends Science Publishers

Keywords: Collagen-like peptides; Directed self-assembly; Recombinant quasi-spider silk protein; Structure characterization

Introduction

Spider silk protein fiber is generated by special glands of certain groups of Arthropoda such as Insecta, Arachnida and Myriapoda. It is one of the best known natural fibers in terms of toughness (Bittencourt, 2016; Humenik *et al.*, 2018). At present, eight kinds of different silk proteins (Dicko *et al.*, 2006) formed by eight kinds of silk glands (not every spider has eight kinds of silk glands at the same time) have been found. The silk protein has four kinds of common motifs: GPGXX, GGX, An/(GA)_n, and spacer. These different motifs determine the different structures and functions of spider silk protein to balance the strength and elasticity of spider silk (Rising *et al.*, 2011).

The distinctive sequence structure of spider silk protein accounts for its unique physicochemical, mechanical, and biological properties (Petzold *et al.*, 2017). The excellent mechanical properties of the spider silk have enhanced its application potential in medical, military, textile, and garment fields, as high-strength materials, such as surgical suture, scaffold, aerospace composite materials, military protective clothing, parachute rope, weaving wheel tire, high-strength nets, and so forth (Chiasson *et al.*, 2016; Thamm and Scheibel, 2017; Kucharczyk *et al.*, 2018). Although the spider silk has broad application prospects, spiders are difficult to tame because of their habit of cannibalism. Therefore, the silkworm rearing, spider silk production and use, as well as researches on spider silk are limited (Xia and Demain, 2010). The development of gene recombination

technology (Weichert *et al.*, 2014; Jansson *et al.*, 2016; Peng *et al.*, 2016) has facilitated the study of the expression of recombinant spider silk protein using a variety of hosts. Meanwhile, recombinant spider silk protein can now be processed into high-performance fibers with varied non-fibrous morphology. Moreover, the molecular weight of the recombinant product has greatly improved. For example, a spider silk protein FLAG was produced in 2016 through intein-based trans-splicing, the molecular weight of this traditionally produced multimer is 460 kDa bigger than before, which remarkably exceeds the natural FLAG protein (Weichert *et al.*, 2016). However, recombination spider silk protein is still ideal for biomedical applications and other fields owing to its excellent biocompatibility and low immunogenicity. Therefore, the production of recombinant spider silk protein using genetic engineering technology has become a significant topic for research (Humenik *et al.*, 2011).

Despite the great progress in the use of various systems for the expression of artificial silk protein, shortcomings still exist: (1) the expression of artificial silk protein gene is not significant compared with that of the natural silk protein gene; (2) Generally, molecular orientation is absent in artificial spider silk proteins; (3) the fibrosis of simulated spider silk cannot be achieved, that is, artificial silk with natural silk fiber properties cannot be made successfully; and (4) the stability of the expression system is a problem, and the expression efficiency is also relatively low (An *et al.*, 2011; Widhe *et al.*, 2012). Due to these problems, the actual applications of spider silk

protein are restricted.

The present study aims at expressing a recombinant quasi-spider silk protein of “ABA” type, so that to avoid the defects of small molecular weight and lacking molecular orientation of the traditional silk protein.

Materials and Methods

Plasmids and Strains

E. coli strain Top10F' and Rosetta (DE3); vector pUC57 and *E. coli* expression vector pET-28a; restriction enzymes *Dra*III, *Van*91I, *Not*I and *Eco*RI; Ex Taq DNA polymerase and T4 DNA ligase; Agarose Gel DNA Purification Kit and MiniBEST Plasmid Purification Kit; DNA Marker DL10000, DNA Marker DL20000 and Protein Marker (Mid. Range); Ampicillin, Kanamycin, and other standard chemicals were bought from Shanghai Sangon (Shanghai, China).

Design of Recombinant Quasi-spider Silk Protein Gene

Literature (Liu *et al.*, 2017) has been used as the reference for the whole process of gene design. According to *Argiope trifasciata* major ampullate spidroin gene (GenBank accession number AH015065) and synthetic construct dragline spider silk protein gene (GenBank accession number AY555585), the monomeric spider silk gene (hereinafter referred to as ‘S’) was devised. It was appropriately modified according to the characteristics of the structure and codon of the gene sequences. With the Garnier method in Antheptot 5.0 software (Institute of Biology and Chemistry of Proteins, France), the protein secondary structure was predicted. Recognition sites of isocaudamers *Van*91I and *Dra*III were located at both ends of the gene, respectively.

Four pieces of single-segment DNA fragments, A1 and A2, were designed. Of these, A1-1 and A1-2 contained *Eco*RI recognition sites, and A2-1 and A2-2 contained *Not*I recognition sites. Genes with collagen-like peptide (Pro-Gly-Pro)_n homopolymeric stretch blocks were designed, with both ends containing isocaudamers *Dra*III and *Van*91I recognition sites. The value of *n* was taken as 15 temporarily because it was impossible to determine the optimum repetition number of the homopolymers. The designed gene was synthesized by the chemical method.

Construction and Screening of *E. coli* Expression Vector pET-28a-TS4T

The whole process of gene construction is shown in Fig. 1. A1S was synthesized and inserted into the *Sma*I site of the pUC57 vector. The new vector was named pUC57-A1S. The A1S fragment (381 bp) was obtained by double cleavage on pUC57-A1S with *Eco*RI and *Van*91I. The pUC57-A1S2 was obtained after connecting the A1S

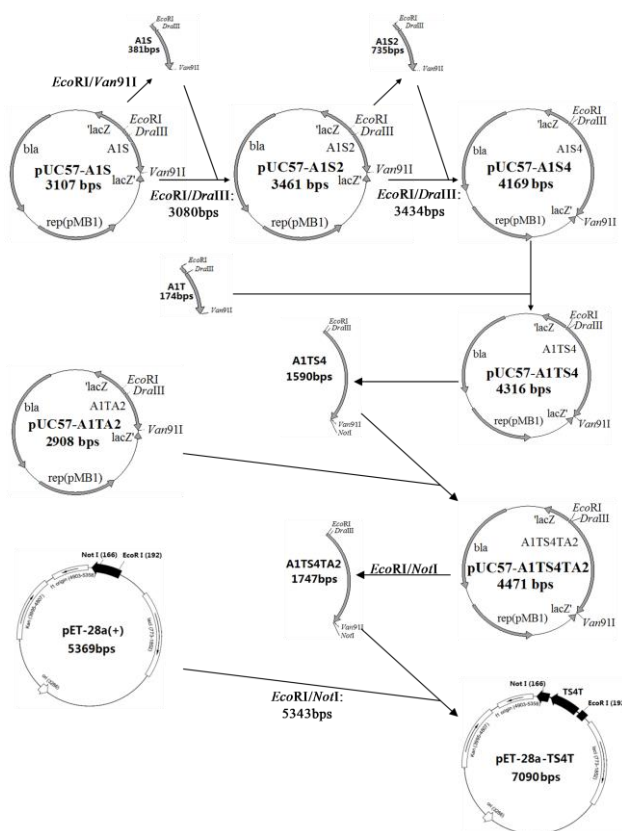


Fig. 1: Construction of recombinant quasi-spider silk protein gene expression vector pET-28a-TS4T

fragment with the product of double digestion on pUC57-A1S with *Eco*RI and *Dra*III. Then, the A1S2 fragment obtained by double digestion on pUC57-A1S2 with *Eco*RI and *Van*91I and the large fragment obtained by double digestion on the same vector with *Eco*RI and *Dra*III were connected. The connection product was transformed into Top10F' to obtain Top10F'/pUC57-A1S4 transformants.

A1TA2 was synthesized and inserted into the *Sma*I site of the pUC57 vector. The new vector was named pUC57-A1TA2. Then, the A1T fragment (174 bp) obtained by double digestion on pUC57-A1TA2 with *Eco*RI and *Van*91I and the large fragment obtained by double enzyme digestion on the pUC57-A1S4 with *Eco*RI and *Dra*III were connected. The connection product was transformed into Top10F' to obtain Top10F'/pUC57-A1TS4 transformants.

The pUC57-A1TS4 vector was digested with *Eco*RI and *Van*91I and the A1TS4 fragment (2298 bp) was obtained. This fragment was connected with the large fragments obtained by double digestion on the pUC57-A1TA2 with *Eco*RI and *Dra*III. The connection product was transformed into Top10F' to obtain Top10F'/pUC57-A1TS4TA2 transformants.

The pUC57-A1TS4TA2 vector was digested with *Not*I and *Eco*RI to obtain the A1TS4TA2 fragment (1747 bp). This fragment was connected with the large fragments

obtained by double digestion on the pET-28a vector with *EcoRI* and *NotI*. The connection product pET-28a-TS4T was transformed into Rosetta(DE3) strain by heat shock treatment. After heat shock transformation, bacterial clones were grown on Luria-Bertani medium plate (including 34 $\mu\text{g/mL}$ chloramphenicol and 30 $\mu\text{g/mL}$ kanamycin). Some clones were picked randomly and cultured in the Luria-Bertani liquid medium (including 34 $\mu\text{g/mL}$ chloramphenicol and 30 $\mu\text{g/mL}$ kanamycin) to produce a resistant single colony.

Expression and Purification of Recombinant Quasi-spider Silk Protein

The genetically engineered *E. coli* were cultured by Isopropyl- β -D-thiogalactoside (IPTG) induction to express the interest protein. Then, the cells and supernatant were isolated by centrifugation at 7155g for 8 min. The bacteria were lysed by ultrasonic cell fragmentation. The lysed cell supernatant was purified by Ni-agarose affinity chromatography (the target protein contained a polyhistidine-tag). The conditions for affinity chromatography were as follows: first loading 5 mL of nickel-iminodiacetic acid (Ni-IDA) agarose resin on the chromatography column and then cleaning the column with the binding buffer 10 times at the flow velocity of 5 mL/min. Then, the sample was loaded on the column, and the penetrating liquid was collected; the flow rate was 2 mL/min. The column was cleaned with 10 times the volume of the binding buffer; the flow rate was 10 mL/min. The wash buffer was used to clean the impurities, and the eluent was collected; the flow rate was 5 mL/min. Then, the eluent was eluted with elution buffer; the flow rate was 2 mL/min. Next, desalination treatment was performed. A certain number of samples were collected and lyophilized. These lyophilized products were used for subsequent analysis and identification.

Sodium Dodecyl Sulfate-polyacrylamide Gel Electrophoresis Analyses

Sodium dodecyl sulfate-polyacrylamide gel electrophoresis (SDS-PAGE) electrophoresis was conducted according to the conventional methods. The concentration of the concentrated and normal gels was 5% and 10%, respectively. The sample was dissolved and the sample buffer was added for electrophoresis. The voltage of the normal and separation gels was 120 V and 200 V, respectively. Coomassie brilliant blue R-250 was used for staining.

Matrix-assisted Laser Desorption/ionization Time-of-flight Mass Spectrometry Analyses

Purified sample was characterized by matrix-assisted laser desorption/ionization time-of-flight mass spectrometry (MALDI-TOF MS) using AB SCIEX 5800 MALDI-TOF/TOF (AB SCIEX, USA). The sample target having

been calibrated by checking its external calibrants, the relative molecular weight of the purified sample was then tested. The original datum were generated by 5800 MALDI-TOF/TOF and were exported using 4000 Series Explorer V 3.5 software (AB SCIEX, USA). With 4% (v/v) trifluoroacetic acid and sinapinic acid dissolved in 30% (v/v) acetonitrile as the matrix, the purified samples were preprocessed with the dried droplet method. The accelerating voltage was 25 kV, and the measurements were made in the positive under linear mode.

Fourier Transform Infrared Spectroscopy

The spectra of purified samples were collected on a Nicolet iS5 Fourier transform infrared (FTIR) spectroscope (Thermo Fisher Scientific, USA) equipped with a deuterated triglycine sulfate detector (DTGS). The solid sample was mixed with KBr in the mass ratio of 1:20. All spectra were recorded at the resolution 4 cm^{-1} and 16 times scanning in the range of 4000–400 cm^{-1} at room temperature.

Circular Dichroism Spectroscopy

The purified sample was dissolved in ultra-pure water with a concentration of 0.1 mg/mL. The measurements were made on a 2BYY-004-0003 spectropolarimeter (APL, England). The path length was 0.1 cm and the spectra were recorded from 190 to 400 nm at room temperature, with a scanning speed of 100 nm/min at a resolution of 0.1 nm.

Results

Identification of *E. coli* Expression Vector pET-28a-TS4T

The plasmids of positive transformants were selected and the extracted pET-28a-TS4T *E. coli* expression vector was digested with *EcoRI/NotI*. As illustrated in Fig. 2, the two fragments were 5.3 and 1.7 kbp, respectively. Therefore, the total actual value was 7.0 kbp. The theoretical value of the two fragments was 1747 and 5343 bp, respectively and the total theoretical value was 7090 bp. Therefore, the actual value was in agreement with the theoretical value.

DNA sequencing of *E. coli* expression vector pET-28a-TS4T was performed by Sangon Biotech (Shanghai) Co., Ltd., and the findings were concordant with the expected results (data not shown).

Detection of Recombinant Quasi-spider Silk Protein Using SDS-PAGE

The interest protein gene was expressed in genetically engineered *E. coli* induced by IPTG. After centrifugation, ultrasonic fragmentation of bacteria and recentrifugation, and the supernatants containing silk protein were collected. The supernatant was then purified with a Ni-agarose affinity

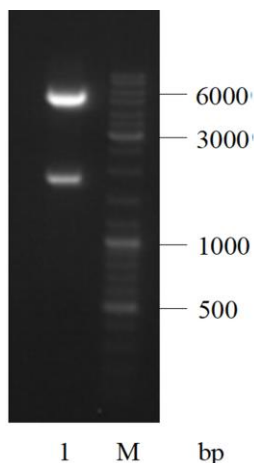


Fig. 2: Verification of pET-28a-TS4T by double-enzyme cleavage method. 1: pET-28a-TS4T (*EcoRI/NorI*); M: DL10000 DNA Marker

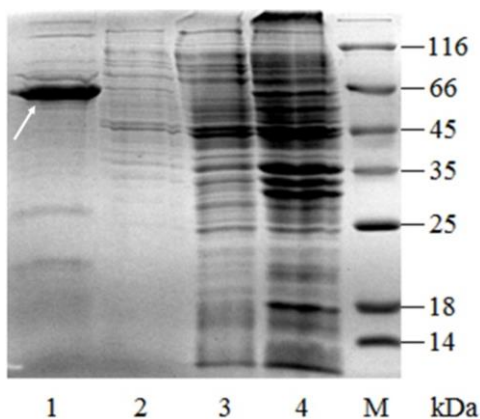


Fig. 3: SDS-PAGE analysis of the recombinant quasi-spider silk protein expression and purification. Lane M, Protein marker, mid-range; lane 1, purified sample; lane 2, eluent; lane 3, penetrating liquid; lane 4, supernatant

chromatography. A certain amount of sample was collected, dialyzed, desalted and freeze-dried to obtain the interest protein. Then, the interest protein was identified.

The SDS-PAGE analysis of purified products is shown in Fig. 3. The results showed that the purity of interest protein bands (marked by a white arrow) obtained by affinity chromatography was 99% (lane 1). The protein was analyzed by using Bio-Rad's Quantity One software (Bio-Rad, USA). The theoretical molecular weight of the interest protein was 52.242 kDa and its apparent molecular weight was found to be about 60.0 kDa, which is actually expected for spider silks because these usually migrate a bit slowly. At the same time, the corresponding bands could be found in the supernatant lane (lane 4) of the corresponding position. These results indicated that the gene construction, expression and purification of interest protein was successful.

MALDI-TOF-MS Analyses

The purified sample was detected by MALDI-TOF-MS analysis so as to get the accurate molecular weight of recombinant quasi-spider silk protein. Fig. 4 shows the results. The exact molecular weight of the interest protein was 52032.46 Da. The designed protein theoretically contained 615 amino acids, its theoretical molecular weight was 52242.93 Da. Obviously, the theoretical molecular weight was extremely close to the actual accurate value.

FTIR and Deconvolved Spectra

The Fourier transform infrared spectroscopy (FTIR) of the prepared sample is shown in Fig. 5. The pure recombinant quasi-spider silk protein displayed peaks at 1636.90 and 1384.71 cm^{-1} , which were characteristic of amide I and II bands, respectively. The amide I absorption was predominantly due to protein amide C=O stretching vibrations, whereas the amide II absorption was accounted for by amide N-H bending vibrations and C-N stretching vibrations. The amide III peak appeared at 1146.25 cm^{-1} , composed of components from C-N stretching and N-H plane bending, as well as absorptions due to wagging vibrations from CH_2 groups. The protein also showed characteristic peaks at 2933.198 and 2857.988 cm^{-1} , which represented the presence of $-\text{CH}_2$ stretching vibrations and $-\text{CH}_2$ flexural vibrations, respectively (Surewicz *et al.*, 1993).

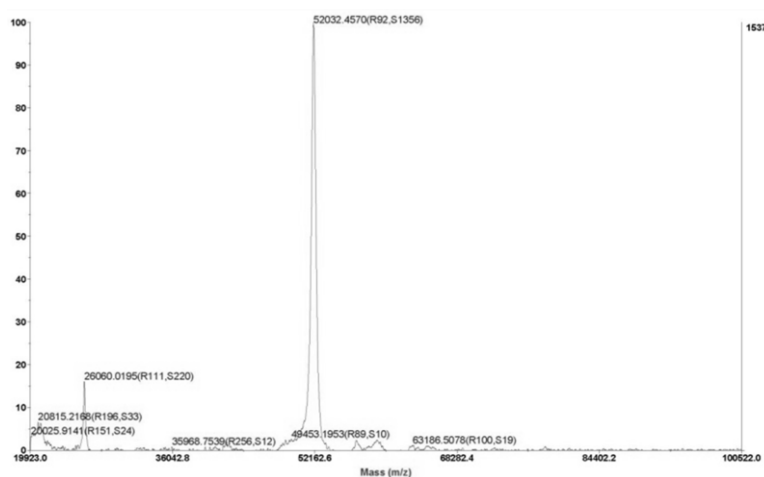
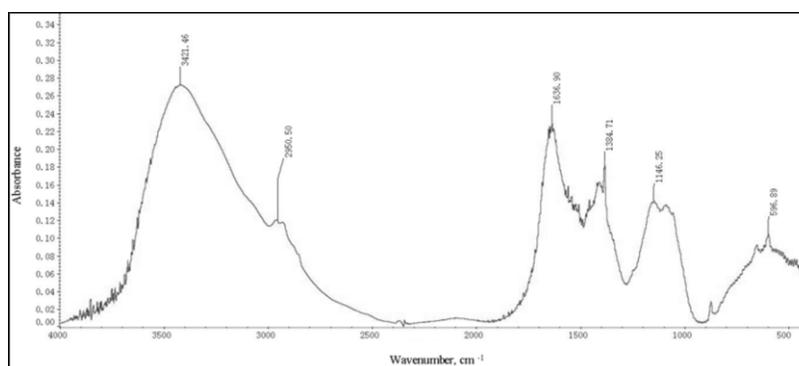
The amide I band, between 1600 and 1700 cm^{-1} , was the most useful and the amide III band was significant for FTIR analysis of the secondary structure of proteins (Mu Yonga *et al.*, 2004). Deconvolution of the amide I and III bands showed the composition of different components in the prepared lyophilized product. The second derivative spectra and curve fitting of the amide I band on the FTIR spectra of interest protein were implemented with PeakFit v 4.12 software (SeaSolve Software Inc., USA). The location of component peaks, peak area and percentage of areas are shown in Fig. 6 and Table 1. The result showed that the interest protein was composed of 31.80% α -helices, 49.62% β -sheets, 18.58% turns, and 0.00% random structures.

Circular Dichroism Spectroscopy

Circular dichroism spectroscopy (Fig. 7) with the detection wavelength of 190–260 nm showed that the α -helices accounted for 12.38%, β -sheets accounted for 40.66%, β -turns accounted for 15.24% and random structures accounted for 31.72%. After the results of the calculation of secondary structure, deconvolution of the amide I band of FTIR spectra and circular dichroism spectroscopy were compared, it was revealed that the proportion of β -sheets was the highest, followed by the proportion of α -helices. Especially, the results of the calculation of secondary structure and deconvolution of the amide I band of FTIR spectra were quite consistent, which,

Table 1: Second derivative and curve fitting results of amide I band of recombinant quasi-spider silk protein

	Peak center (cm ⁻¹)	Peak area	Ratio (%)	Assignment
1	1615.0728	0.2526969	9.30	β-sheets
2	1625.8639	0.4986078	18.35	β-sheets
3	1636.8718	0.5968982	21.97	β-sheets
4	1646.6835	0.4190701	15.43	α-helices
5	1654.4773	0.4446752	16.37	α-helices
6	1663.1517	0.2928778	10.78	β- turns
7	1672.1264	0.2119610	7.80	β- turns

**Fig. 4:** Mass spectrographic analysis of recombinant quasi-spider silk protein**Fig. 5:** FTIR spectra analysis of recombinant quasi-spider silk protein

in turn, was in consonance with the features of natural spider silk protein. Therefore, it could be concluded that the interest protein and natural spider silk protein had similar structural characteristics. However, although the protein contains collagen blocks, there is no way to observe the triplehelix structure through circular dichroism spectroscopy.

Discussion

A recombinant quasi-spider silk protein with directional self-assembly function was generated based on the complete artificial synthetic gene sequence in this study. This interest

protein was a triblock copolymer of “ABA” type which fused collagen-like peptides with spider silk protein. It had the properties of directional self-assembly to form a supramolecular structure (Werten *et al.*, 2009), which could ensure that the artificial silk fibers met the requirements in terms of molecular weight and rendered the interest protein a definite molecular orientation. Moreover, the fibers were strengthened with the help of chemical bonds formed in the self-assembly with end-to-end alignment.

A recombinant quasi-spider silk protein gene vector was constructed by using a pair of isocaudamers with monomer tandem repeating strategy carried out on spider

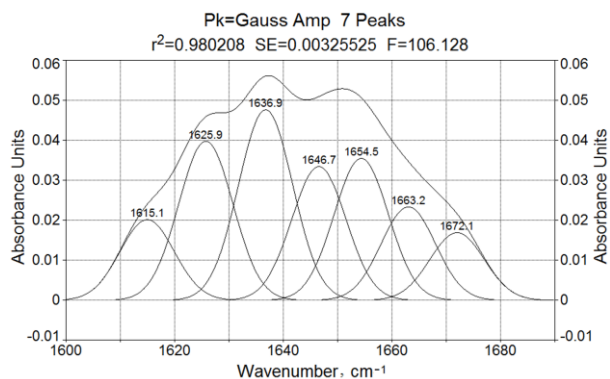


Fig. 6: Deconvolution of the amide I band of FTIR spectra of recombinant quasi-spider silk protein

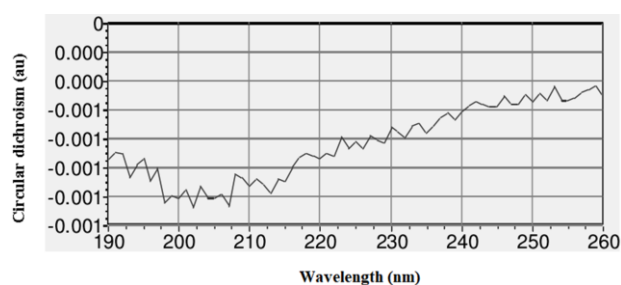


Fig. 7: Circular dichroism spectroscopy of recombinant quasi-spider silk protein

silk protein monomer gene and collagen-like peptide gene. Finally, the interest protein gene was expressed successfully in *E. coli*. This method for constructing the interest protein gene was highly advantageous compared with the technique realizing gene duplication by polymerase chain reaction. First, the amino acid sequence of spider silk protein can be changed more flexibly with this method to optimize the function of the interest protein in the premise of maintaining the natural silk protein sequence. Second, the best-performance structure of the interest protein could be determined by changing the length of collagen-like peptide (Pro-Gly-Pro)_n homopolymeric stretch blocks (Werthen *et al.*, 2009). Third, the method could realize the tandem connection of the interest protein gene with any repeated number by preparing tandem duplication gene recombinant plasmid, so that to realize the expression of high-molecular-weight interest protein close to that of natural spider silk protein.

This study provided a new technology for preparing new-style spider silk protein by protein engineering and gene recombination technology. The results showed that the construction of the interest protein was successful. Further research on the structure and chemical properties of the interest protein is still in progress, and further studies are needed to find a good fiber-forming technology to realize the purpose of applying the interest protein in the biomedical engineering field.

Conclusion

A 52032.46-Da recombinant quasi-spider silk protein was efficiently produced in *E. coli*. MALDI-TOF-MS, FTIR spectroscopy and circular dichroism spectroscopy analyses showed that the structural characteristics of the interest protein were similar to those of natural spider silk protein. This interest protein consisted of triblock copolymers of terminal (Pro-Gly-Pro)₁₅ blocks and an intervening block of spider silk protein. Based on the data available, we propose the hypothesis that the end blocks could form collagen-like triple helices to ensure that the interest protein could constitute a supramolecular structure to meet the molecular orientation and molecular weight requirements of synthetic spider silk fibers in the transversion of silk fiber formation. However, this conjecture still calls for further verification.

Acknowledgments

We acknowledge the financial supports of the National Natural Science Foundation of China under Grant No. 31360228.

References

- An, B., M.B. Hinman, G.P. Holland, J.L. Yarger and R.V. Lewis, 2011. Inducing β -sheets formation in synthetic spider silk fibers by aqueous post-spin stretching. *Biomacromolecules*, 12: 2375–2381
- Bittencourt, D.M.D.C., 2016. Spider silks and their biotechnological applications. In: *Short Views on Insect Genomics and Proteomics, Insect Proteomics*, Vol. 2, pp: 211–227. Raman, C., M.R. Goldsmith and T.A. Agunbiade (eds.). Springer International Publishing, Cham, Switzerland
- Chiasson, R., M. Hasan, Q.A. Nazer, O.C. Farokhzad and N. Kamaly, 2016. The use of silk in nanomedicine applications. In: *Nanomedicine*, pp: 245–278. Howard, K.A., T. Vorup-Jensen and D. Peer (eds.). Springer, New York, USA
- Dicko, C., J.M. Kenney and F. Vollrath, 2006. Beta-silks: enhancing and controlling aggregation. *Adv. Protein Chem.*, 73: 17–53
- Humenik, M., M. Mohrand and T. Scheibel, 2018. Self-assembly of spider silk-fusion proteins comprising enzymatic and fluorescence activity. *Bioconj. Chem.*, 29: 898–904
- Humenik, M., A.M. Smith and T. Scheibel, 2011. Recombinant spider silks-biopolymers with potential for future applications. *Polymers*, 3: 640–661
- Jansson, R., C.H. Lau, T. Ishida, M. Ramström, M. Sandgren and M. Hedhammar, 2016. Functionalized silk assembled from a recombinant spider silk fusion protein (Z-4RepCT) produced in the methylotrophic yeast *Pichia pastoris*. *Biotechnol. J.*, 11: 687–699
- Kucharczyk, K., M. Weiss, K. Jastrzebska, M. Luczak, A. Ptak, M. Kozak, A. Mackiewicz and H. Dams-Kozłowska, 2018. Bioengineering the spider silk sequence to modify its affinity for drugs. *Intl. J. Nanomed.*, 13: 4247–4261
- Liu, B., T. Wang, L. Xiao, G. Zhang, G. Li, J. Luo and X. Liu, 2017. A directed self-assembly quasi-spider silk protein expressed in *Pichia pastoris*. *Biotechnol. Biotechnol. Equip.*, 32: 451–461
- Muyonga, J.H., C.G.B. Cole and K.G. Duodu, 2004. Fourier transform infrared (FTIR) spectroscopic study of acid soluble collagen and gelatin from skins and bones of young and adult Nile perch (*Lates niloticus*). *Food Chem.*, 86: 325–332
- Peng, C.A., J. Russo, C. Gravgard, H. McCartney, W. Gaines and W.R.M. Jr, 2016. Spider silk-like proteins derived from transgenic *Nicotiana tabacum*. *Trans. Res.*, 25: 517–526

- Petzold, J., T.B. Aigner, F. Touska, K. Zimmermann, T. Scheibel and F.B. Engel, 2017. Surface features of recombinant spider silk protein eADF4(κ 16)-made materials are well-suited for cardiac tissue engineering. *Adv. Funct. Mater.*, 27: 1–11
- Rising, A., M. Widhe, J. Johansson and M. Hedhammar, 2011. Spider silk proteins: recent advances in recombinant production, structure-function relationships and biomedical applications. *Cell. Mol. Life Sci.*, 68: 169–184
- Surewicz, W.K., H.H. Mantsch and D. Chapman, 1993. Determination of protein secondary structure by Fourier transform infrared spectroscopy: a critical assessment. *Biochemistry*, 32: 389–394
- Thamm, C. and T. Scheibel, 2017. Recombinant production, characterization and fiber spinning of an engineered short major ampullate spidroin (MaSp1s). *Biomacromolecules*, 18: 1365–1372
- Weichert, N., V. Hauptmann, C. Helmold and U. Conrad, 2016. Seed-specific expression of spider silk protein multimers causes long-term stability. *Front. Plant Sci.*, 7: 6
- Weichert, N., V. Hauptmann, M. Menzel, K. Schallau, P. Gunkel, T.C. Hertel, M. Pietzsch, U. Spohn and U. Conrad, 2014. Transglutamination allows production and characterization of native-sized ELPylated spider silk proteins from transgenic plants. *Plant Biotechnol. J.*, 12: 265–275
- Werten, M.W., H. Teles, A.P. Moers, E.J. Wolbert, J. Sprakel, G. Eggink and F.A.D. Wolf, 2009. Precision gels from collagen-inspired triblock copolymers. *Biomacromolecules*, 10: 1106–1113
- Widhe, M., J. Johansson, M. Hedhammar and A. Rising, 2012. Current progress and limitations of spider silk for biomedical applications. *Biopolymers*, 97: 468–478
- Xia, X.X. and A.L. Demain, 2010. Native-sized recombinant spider silk protein produced in metabolically engineered *Escherichia coli* results in a strong fiber. *Proc. Natl. Acad. Sci. USA*, 107: 14059–14063

(Received 14 September 2018; Accepted 30 October 2018)